

Quantum noise reduction in singly resonant optical devices

C. Cabrillo,* J. L. Roldán, and P. García-Fernández*

Instituto de Estructura de la Materia, Consejo Superior de Investigaciones Científicas, Serrano 123, 28006 Madrid, Spain

Received April 26, 1999; revised manuscript received September 20, 1999

Quantum noise in a model of singly resonant frequency doubling, including phase mismatch and driving in the harmonic mode, is analyzed. The use of a nonlinear normalization allows us to disentangle in the spectra the squeezing induced by the system dynamics from the deleterious effect of the noise coming from the various inputs. The physical insight gained permits the elaboration of general criteria to optimize noise-suppression performance. The subsequent application to the specific system here addressed reveals excellent squeezing behavior. In particular, unlimited degrees of squeezing in the harmonic mode are possible by means of an adequate phase mismatch or driving in the harmonic mode. This is in contrast with the standard phase-matched second-harmonic generation in which the squeezing is limited to 1/9. The applicability of the model, as well as possible experimental implementations, is extensively discussed. © 2000 Optical Society of America [S0740-3224(00)00103-X]

OCIS codes: 270.0270, 270.6570, 270.2500.

1. INTRODUCTION

Second-harmonic generation (SHG) has been established as a means for squeezed-light generation.¹⁻⁷ The preferred experimental setup has been the doubly resonant configuration that in principle may attain arbitrarily large squeezing. However, practical implementation of this scheme has been hampered by technical difficulties owing to the need for keeping both modes at resonance. In fact, double resonance has been achieved for only a short lapse of time (few seconds) despite the development of ingenious stabilizing procedures³ (this kind of experimental delicacy is hardly surprising when one deals with the generation of nonclassical states of light). In view of such difficulties, some experimental efforts have been recently redirected toward singly resonant configurations.⁴⁻⁶ Although maximum noise suppression is there limited to 90%,⁴ the efforts resulted in stable squeezed-light sources with degrees of squeezing surpassing even those reported for the doubly resonant counterparts.⁶ This evolution highlights the importance of reducing to a minimum the technical demands associated with new proposals in this challenging field.

At the same time, singly resonant optical parametric oscillation (OPO), the most successful method to squeeze the vacuum,^{8,9} has been generalized to singly resonant optical parametric amplification; i.e., a laser driving in the harmonic mode has been added, again showing extraordinary stability at rather high noise-suppression values in the fundamental mode.¹⁰ Although the squeezed beams are in this case much less intense than in the SHG counterpart, this setup permits control of the phase of the squeezed quadrature. This control allowed the performance of a tantalizing demonstration, using quantum state tomography, of the different kinds of squeezed states.¹¹

In view of this experimental success, it seems timely to

extend the quantum mechanical model beyond the pure phase-matched cases. More specifically, we address here quantum noise reduction in an extension of the conventional singly resonant SHG to include a coherent input in the harmonic mode as well as phase mismatch between the interacting waves.

Also, an increasing number of papers have studied quantum noise in systems that combine different kinds of nonlinearities (see, for instance, Refs. 12–16 for some recent contributions). In particular, the combination of $\chi^{(2)}$ with Kerr-like $\chi^{(3)}$ nonlinearities in cw cavity systems has been extensively studied,^{15,17-24} up to the point of deriving exact full quantum results that show the emergence of tristability not present in the classical counterpart.²⁴ With respect to the squeezing performance, results appear as quite promising, at least in degenerate doubly resonant configurations.^{15,22} The simplest system from the implementation point of view, combining these two kinds of nonlinearities, is probably a singly resonant second-order nonlinear system with phase mismatch between the interacting waves, as then, by virtue of the cascading effect, an effective Kerr-like third-order nonlinearity appears.

In the quest of a strong noise reduction through the parameter space, we want analytical expressions for which we shall use standard linearization procedures. Inside the linear approximation, perfect squeezing is possible at dynamic instability points. We use this fact to find optimum working points showing maximum squeezing. They are, however, artifactual, since the linear approximation breaks down at the instabilities. Usually the squeezing behavior with respect to some relevant parameter is studied along a path in the parameter space that corresponds to constant values of the remaining parameters. Instead, we will study it along a path that always yields the maximum squeezing available. The optimum working point will be somewhere along these optimum

paths before reaching an instability. Thus these paths will guide the experimentalist toward the optimum working point in the experimental setup. By means of an adequate normalization, the system dynamics responsible for the squeezing will be isolated from the static contributions to the noise coming from the different inputs. This simplifies the analysis enough to allow a characterization of the optimum paths.

Another crucial issue that appears when we deal with the squeezing performance of a system is the election of the most relevant parameter for comparing the different configurations. There is no universal criterion to determine the squeezing efficiency of a given device. An efficient setup regarding power consumption, i.e., when compared with fixed input power, could well be deceptive when compared with the same output power and may be inadequate for some spectroscopic applications. However, within the state of the art of the present squeezed-light generators, the main concern is to improve the squeezing figures themselves, other considerations being of less importance. Under this perspective, probably the parameter of utmost importance as far as cw resonant systems are concerned is the energy load inside the cavity. The usual causes of squeezing degradation such as blue-light-induced red absorption come from too large mean photon numbers inside the cavity; this can significantly degrade the optical response of the material at the relevant frequencies. These considerations will lead us to define another normalization that is at this time useful for evaluating the squeezing efficiency with respect to the intracavity photon number.

The paper is organized as follows. In Section 2 the quantum mechanical model is presented. In Section 3 the evolution equations are linearized, the fixed points of the dynamical system are obtained, and their stability is studied. Section 4 gives all the formulas regarding quantum noise spectra in the system. In Section 5 an approach to singly resonant systems is developed that allows the definition of criteria to characterize the optimum paths. These criteria are subsequently applied to the specific case addressed here. Finally, the limits of the model and possible implementations are thoroughly discussed in Section 6; a summary of the most relevant results obtained concludes the article.

2. QUANTUM MECHANICAL MODEL

The system we want to address consists of a second-order nonlinear medium coupling two modes of frequency ω (fundamental) and 2ω (harmonic) that is placed inside a ring cavity resonant only with the fundamental mode. We will also assume just one input–output mirror of finite reflectivity. The effect of phase mismatch occurring when only the fundamental mode is driven has been experimentally studied in Ref. 25, in which bistability induced by cascading was demonstrated. The classical evolution equation of the fundamental mode, α , as given in Ref. 25, reads

$$d\alpha/dt = -[\gamma + i\delta + \nu K(\Delta k)|\alpha|^2]\alpha + \sqrt{2}\gamma_c\alpha_{\text{in}}. \quad (2.1)$$

The nonlinear coupling depends on the wave-vector mismatch $\Delta k = k(2\omega) - k(\omega)$ as

$$K(\Delta k) = 2\int_0^{L_m} \int_0^z u^*(\Delta k, z)u(\Delta k, z')dz' dz/L_m^2,$$

where L_m is the length of the nonlinear medium, $u(k, z)$ is the spatial dependence of the resonator mode, and ν is proportional to the second-order nonlinear susceptibility (see below). Splitting $K(\Delta k)$ into its real and imaginary parts, we can recast Eq. (2.1) as

$$d\alpha/dt = -[\gamma + \mu|\alpha|^2 + i(\delta + \Gamma|\alpha|^2)]\alpha + \sqrt{2}\gamma_c\alpha_{\text{in}}. \quad (2.2)$$

For a plane-wave geometry,

$$\mu \equiv \nu K_r(\Delta k) = \nu \left(\text{sinc} \frac{\Delta k L_m}{2} \right)^2, \quad (2.3a)$$

$$\Gamma \equiv \nu K_i(\Delta k) = \frac{2\nu}{\Delta k L_m} \left(\text{sinc} \frac{\Delta k L_m}{2} \cos \frac{\Delta k L_m}{2} - 1 \right), \quad (2.3b)$$

where $K_r(\Delta k)$ and $K_i(\Delta k)$ denote the real and imaginary part of $K(\Delta k)$, respectively. In this way the nonlinear dynamics is divided into a nonlinear absorption (the up-conversion of photons) and a nonlinear dispersion (the cascading effect; see below). The behavior of both parameters with $\Delta k L_m$ are shown in Fig. 1. Note that for any finite $\Delta k L_m$ the nonlinear dispersion is also finite and the frequency doubling vanishes at multiples of $\mp\pi$. When this happens, the harmonic mode passes through the cavity with no net effect, although the fundamental mode experiences a nonlinear phase shift. During a round trip, the fundamental mode is upconverted to the harmonic mode along half of the interaction length and is downconverted back to the fundamental mode in the second half, exactly compensating the gain of the first half. But during the process the fundamental mode changes its phase by an amount proportional to the number of photons upconverted and downconverted. This is the so-called cascading effect. This microscopic process is hidden in the present formulation, for which the time derivative is understood in the “coarse grain” sense, and the round-trip time is considered infinitesimal. Many of the results obtained here are equally valid irrespective of the origin of the nonlinear absorption and dispersion, so that we shall use μ and Γ without arguments.

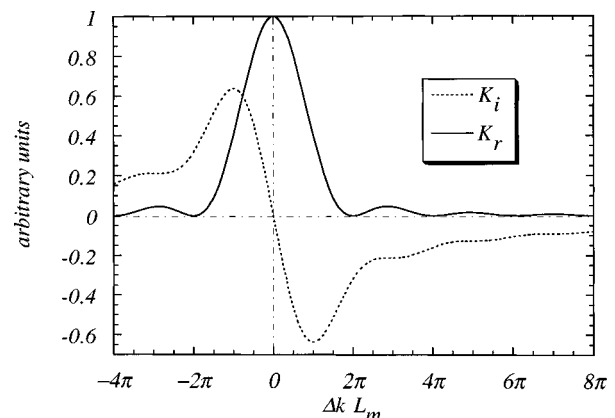


Fig. 1. Dependence of K_i and K_r with respect to the phase mismatch.

Quantization of Eq. (2.2) is then accomplished independently for each effect. We use the two-photon model proposed in Ref. 26 for nonlinear absorption and account for nonlinear dispersion by a fourth-order Hamiltonian, $H = (\hbar\Gamma/2)a^{\dagger 2}a^2$ as in the standard theory of the optical Kerr effect. It represents a Hamiltonian modification of the two-photon absorption model so that the quantum mechanical equation reads

$$\begin{aligned} \frac{da}{dt} = & -[\gamma + i\delta + (\mu + i\Gamma)a^{\dagger}a]a \\ & + 2\sqrt{\mu}a^{\dagger}b_{\text{in}} + \sqrt{2\gamma_c}a_{\text{in}} + \sqrt{2\gamma_s}w_{\text{in}}, \end{aligned} \quad (2.4)$$

where Latin characters denote the annihilation operators for the corresponding classical (Greek characters) modes. Two extra terms not present in the classical analog appear, namely, a white-noise input, w_{in} , accounting for the fluctuations induced by the scattering and the absorption in the crystal ($\gamma_s = \gamma - \gamma_c$), and a parametric amplification term coming from the, classically empty, incoming harmonic mode b_{in} . Equation (2.4) is complemented with the boundary conditions⁴

$$a_{\text{out}} = \sqrt{2\gamma_c}a - a_{\text{in}}, \quad (2.5a)$$

$$b_{\text{out}} = \sqrt{\mu}a^2 - b_{\text{in}}, \quad (2.5b)$$

from which the output spectra can be computed. Input fields are assumed to be in coherent states. In particular, by allowing a coherent state different from the vacuum for the incoming harmonic mode, we generalize the system to the case of driving both modes. We shall also assume zero temperature for the white noise (i.e., vacuum noise), an excellent approximation at optical frequencies. In the case $\Gamma = \delta = 0$, the squeezing properties and the applicability to quantum nondemolition measurements of this system have been studied in detail in Ref. 27.

In Eq. (2.4) we can identify three different processes leading to squeezing. First, the upconversion of photons to a nonresonant mode gives rise to an effective two-photon absorption (the term $\mu a^{\dagger}a$). Second, the nonlinear phase shift (or self-phase modulation) induced by cascading (the term $i\Gamma a^{\dagger}a$). Finally, when there is a coherent component of the input harmonic mode, a parametric amplification below threshold (the term $2\sqrt{\mu}b_{\text{in}}$) also takes place. Because of the nonresonant character of the harmonic mode, it cannot appear isolated but always appears with a concomitant two-photon absorption.

The used definitions for the creation operators give the following relations with the usual experimental parameters (see Appendix in Ref. 27): The input and output powers are $P_{\omega, \text{in/out}} = \hbar\omega\langle a_{\text{in/out}}^{\dagger}a_{\text{in/out}} \rangle$ and $P_{2\omega, \text{in/out}} = \hbar 2\omega\langle b_{\text{in/out}}^{\dagger}b_{\text{in/out}} \rangle$; the circulating power is $\hbar\omega\langle a^{\dagger}a \rangle/\tau$, where τ is the round-trip time and $2\tau^2\nu/\hbar\omega$ is the single-pass power-conversion efficiency (in W^{-1}).

3. LINEARIZED EVOLUTION EQUATIONS AND LINEAR STABILITY ANALYSIS

Defining fluctuation operators as

$$\delta a = a - \alpha, \quad (3.1a)$$

$$\delta a_{\text{in,out}} = a_{\text{in,out}} - \alpha_{\text{in,out}}, \quad (3.1b)$$

$$\delta b_{\text{in,out}} = b_{\text{in,out}} - \beta_{\text{in,out}}, \quad (3.1c)$$

we find that a linearization of Eqs. (2.4) and (2.5) yields

$$\begin{aligned} \frac{d\delta a}{dt} = & -[\gamma + i\delta + 2(\mu + i\Gamma)|\alpha|^2]\delta a \\ & + [2\sqrt{\mu}\beta_{\text{in}} - (\mu + i\Gamma)\alpha^2]\delta a^{\dagger} + 2\sqrt{\mu}\alpha^*\delta b_{\text{in}} \\ & + \sqrt{2\gamma_c}\delta a_{\text{in}} + \sqrt{2\gamma_s}w_{\text{in}}, \end{aligned} \quad (3.2)$$

$$\delta a_{\text{out}} = \sqrt{2\gamma_c}\delta a - \delta a_{\text{in}}, \quad (3.3a)$$

$$\delta b_{\text{out}} = 2\alpha\sqrt{\mu}\delta a - \delta b_{\text{in}}, \quad (3.3b)$$

where $\alpha_{\text{in,out}}$, $\beta_{\text{in,out}}$ are the mean values of the corresponding input and output modes and α is a stable fixed point of the classical counterpart of Eq. (2.4); i.e.,

$$\begin{aligned} \frac{d\alpha}{dt} = & -[\gamma + i\delta + (\mu + i\Gamma)|\alpha|^2]\alpha \\ & + 2\sqrt{\mu}\alpha^*\beta_{\text{in}} + \sqrt{2\gamma_c}\alpha_{\text{in}}. \end{aligned} \quad (3.4)$$

Equating the left-hand side of Eq. (3.4) to zero, a state equation for the fixed points is obtained, namely,

$$\alpha = \frac{\sqrt{2\gamma_c}\{[\gamma + \mu n - i(\delta + \Gamma n)]\alpha_{\text{in}} + 2\sqrt{\mu}\beta_{\text{in}}\alpha_{\text{in}}^*\}}{(\gamma + \mu n)^2 + (\delta + \Gamma n)^2 - 4\mu|\beta_{\text{in}}|^2}, \quad (3.5)$$

with $n = |\alpha|^2$. Let θ , θ_{in} , and φ_{in} be the phases of α , α_{in} , and β_{in} , respectively. Then by dividing both sides of Eq. (3.5) by $\exp(i\varphi_{\text{in}}/2)$, we obtain

$$\begin{aligned} |\alpha| \exp[i(\theta - \varphi_{\text{in}}/2)] [(\gamma + \mu n)^2 + (\delta + \Gamma n)^2 - 4\mu|\beta_{\text{in}}|^2] \\ = |\alpha_{\text{in}}| \sqrt{2\gamma_c} \{[\gamma + \mu n - i(\delta + \Gamma n)] \\ \times \exp[i(\theta_{\text{in}} - \varphi_{\text{in}}/2)] + 2\sqrt{\mu}|\beta_{\text{in}}| \\ \times \exp[-i(\theta_{\text{in}} - \varphi_{\text{in}}/2)]\}. \end{aligned} \quad (3.6)$$

Taking the squared modulus on both sides, we obtain a quintic equation for n :

$$\begin{aligned} 0 = & n[(\gamma + \mu n)^2 + (\delta + \Gamma n)^2 - 4\mu|\beta_{\text{in}}|^2]^2 \\ & - 2\gamma_c|\alpha_{\text{in}}|^2\{(\gamma + \mu n)^2 + (\delta + \Gamma n)^2 + 4\mu|\beta_{\text{in}}|^2 \\ & + 4\sqrt{\mu}|\beta_{\text{in}}|[(\gamma + \mu n)\cos(2\theta_{\text{in}} - \varphi_{\text{in}}) \\ & + (\delta + \Gamma n)\sin(2\theta_{\text{in}} - \varphi_{\text{in}})]\}. \end{aligned} \quad (3.7)$$

The real and the imaginary parts of Eq. (3.6) determine the $\sin(\theta - \varphi_{\text{in}}/2)$ and $\cos(\theta - \varphi_{\text{in}}/2)$ as functions of the solutions of Eq. (3.7):

$$\cos(\theta - \varphi_{\text{in}}/2) = \frac{|\alpha_{\text{in}}| \sqrt{2\gamma_c} (\gamma + \mu n + 2\sqrt{\mu}|\beta_{\text{in}}|) \cos(\theta_{\text{in}} - \varphi_{\text{in}}/2) + (\delta + \Gamma n) \sin(\theta_{\text{in}} - \varphi_{\text{in}}/2)}{(\gamma + \mu n)^2 + (\delta + \Gamma n)^2 - 4\mu|\beta_{\text{in}}|^2}, \quad (3.8a)$$

$$\sin(\theta - \varphi_{\text{in}}/2) = \frac{|\alpha_{\text{in}}| \sqrt{2\gamma_c} (\gamma + \mu n - 2\sqrt{\mu}|\beta_{\text{in}}|) \sin(\theta_{\text{in}} - \varphi_{\text{in}}/2) - (\delta + \Gamma n) \cos(\theta_{\text{in}} - \varphi_{\text{in}}/2)}{(\gamma + \mu n)^2 + (\delta + \Gamma n)^2 - 4\mu|\beta_{\text{in}}|^2}. \quad (3.8b)$$

Equation (3.7) allows the numerical calculation of the fixed points given the input fields. But it can also be interpreted as a linear equation for $|\alpha_{\text{in}}|^2$ whose solution is

$$2\gamma_c |\alpha_{\text{in}}|^2 = \frac{n[(\gamma + \mu n)^2 + (\delta + \Gamma n)^2 - 4\mu|\beta_{\text{in}}|^2]^2}{|\gamma + \mu n + 2\sqrt{\mu}|\beta_{\text{in}}|\exp[i(2\theta_{\text{in}} - \varphi_{\text{in}})]|^2 + 4\sqrt{\mu}|\beta_{\text{in}}|(\delta + \Gamma n)\sin(2\theta_{\text{in}} - \varphi_{\text{in}})}. \quad (3.9)$$

The positive character of the right-hand side is not always guaranteed and therefore a real positive n is not possible for every value of the parameters. Note, however, that in the cases in which this happens a simultaneous change of the sign of δ and Γ yields a consistent set of parameter values. As we shall see, this fact will have useful consequences for the analysis of the quantum noise behavior in the system.

The stability of the fixed points is governed by the real part of the eigenvalues of the drift matrix that is associated with the linearized evolution equation [Eq. (3.2)]. Very simple algebra yields

$$\lambda_{\pm} = -(\gamma + 2\mu n) \pm [(\mu + i\Gamma)\alpha^2 - 2\sqrt{\mu}|\beta_{\text{in}}|^2 - (\delta + 2\Gamma n)^2]^{1/2}. \quad (3.10)$$

Provided that the real part of both eigenvalues is negative, the fixed point will be stable. With respect to the phase-matched SHG case ($\Gamma = 0$ and $\beta_{\text{in}} = 0$, always stable), finite values of Γ and simultaneously of δ can destabilize the system. A finite β_{in} , on the other hand, can promote instability, depending on its relative phase with respect to α , the case of $\theta - \varphi_{\text{in}}/2 = \pm\pi/2$ maximizing the effect. All of these new instabilities, however, correspond to zero eigenvalues without a finite imaginary part. In other words, in contrast to the doubly resonant SHG, there is no Hopf bifurcation leading to self-pulsing behavior.

4. SQUEEZING SPECTRA

For a given quadrature of the electric field, $X_{\phi}^{\text{out}}(t) \equiv a_{\text{out}}(t)\exp(-i\phi) + a_{\text{out}}^{\dagger}(t)\exp(i\phi)$, the squeezing spectrum is simply the noise spectrum of such a quantity; i.e.,

$$S(\omega) = C \int_{-\infty}^{\infty} \langle \delta X_{\phi}^{\text{out}}(t) \delta X_{\phi}^{\text{out}}(t + \tau) \exp(-i\omega\tau) d\tau \rangle \equiv C \langle \delta X_{\phi}^{\text{out}}(\omega) \delta X_{\phi}^{\text{out}}(-\omega) \rangle, \quad (4.1)$$

where C is some normalization constant and the averages are assumed stationary. As a function of the annihilation and creation operators, Eq. (4.1) is rewritten as

$$S(\omega) = C[\langle \delta a_{\text{out}}^{\dagger}(\omega) \delta a_{\text{out}}(-\omega) \rangle + \text{Re}\{\exp(-i2\phi) \langle \delta a_{\text{out}}(\omega) \delta a_{\text{out}}(-\omega) \rangle\}], \quad (4.2)$$

where use has been made of the stationary character of the average and Re denotes real part. From this expression it is evident that the noise is minimized, and therefore the squeezing effect is maximized for a quadrature phase such as

$$S(\omega) = C[\langle \delta a_{\text{out}}^{\dagger}(\omega) \delta a_{\text{out}}(-\omega) \rangle - |\langle \delta a_{\text{out}}(\omega) \delta a_{\text{out}}(-\omega) \rangle|], \quad (4.3)$$

corresponding to a phase

$$\phi_{\text{opt}} = \frac{\epsilon(\omega) - \pi}{2}, \quad (4.4)$$

where $\epsilon(\omega)$ is the phase of $\langle \delta a_{\text{out}}(\omega) \delta a_{\text{out}}(-\omega) \rangle$. The spectrum of the conjugate quadrature [i.e., with a phase $\epsilon(\omega)/2$] corresponds to a plus sign in Eq. (4.3) and by virtue of the Heisenberg principle it shows excess noise above the vacuum. Taking $C = 1$ (corresponding to vacuum noise units) and splitting Eq. (4.3) into a vacuum noise component plus a normally ordered part, we finally arrive at

$$S_{-,+}(\omega) = 1 + \langle : \delta a_{\text{out}}^{\dagger}(\omega) \delta a_{\text{out}}(-\omega) : \rangle \mp |\langle : \delta a_{\text{out}}(\omega) \delta a_{\text{out}}(-\omega) : \rangle|, \quad (4.5)$$

for both the squeezing and the stretching spectra. After tedious but simple algebra, the spectra of the fundamental and second-harmonic modes can be written as

$$S_{-,+}^a(\omega) = 1 + 4\gamma_c |B| \frac{N_{-,+}}{D}, \quad (4.6a)$$

$$S_{-,+}^b(\omega) = 1 + 8\mu n |B| \frac{N_{-,+}}{D}, \quad (4.6b)$$

where $B = 2\sqrt{\mu}\beta_{\text{in}} - (\mu + i\Gamma)\alpha^2$ and

$$N_{-,+} = 2|B|(\gamma + 2\mu n) \mp \sqrt{[(\gamma + 2\mu n)^2 - (\delta + 2\Gamma n)^2 + |B|^2 + \omega^2]^2 + 4(\gamma + 2\mu n)^2(\delta + 2\Gamma n)^2}, \quad (4.7a)$$

$$D = [(\gamma + 2\mu n)^2 + (\delta + 2\Gamma n)^2 - |B|^2 - \omega^2]^2 + 4(\gamma + 2\mu n)^2\omega^2. \quad (4.7b)$$

The correlations defining the squeezing phase $\epsilon(\omega)$ are given by

$$\begin{aligned} \langle \delta a_{\text{out}}(\omega) \delta a_{\text{out}}(-\omega) \rangle \\ = 4\gamma_c B[\omega^2 + |B|^2 + (\gamma + 2\mu n)^2 - (\delta + 2\Gamma n)^2 \\ + i2(\gamma + 2\mu n)(\delta + 2\Gamma n)]/D, \end{aligned} \quad (4.8a)$$

$$\begin{aligned} \langle \delta b_{\text{out}}(\omega) \delta b_{\text{out}}(-\omega) \rangle \\ = 8\mu\alpha^2 B[\omega^2 + |B|^2 + (\gamma + 2\mu n)^2 - (\delta + 2\Gamma n)^2 \\ + i2(\gamma + 2\mu n)(\delta + 2\Gamma n)]/D. \end{aligned} \quad (4.8b)$$

The trigonometric equations for the corresponding phases are quite complicated. However, an interesting consequence can be drawn directly from Eqs. (4.8); that is, for detunings such as $\delta + 2\Gamma n = 0$, the phases are independent of ω , equaling those of B and $\alpha^2 B$, respectively.

5. SQUEEZING PERFORMANCE

As mentioned in the Introduction, before specific assessment of the quantum noise performance, we will present the formulas in more detail (mainly by adequate normalizations) to gain physical insight that will ease our task.

A. Some General Results Concerning Singly Resonant Systems

Let us begin by defining a nonlinear and a total decay rate as $\gamma_{nl} \equiv 2\mu n$ and $\gamma_t \equiv \gamma + \gamma_{nl}$, respectively. We shall scale the evolution with this total decay rate, defining a dimensionless time $\tau \equiv \gamma_t t$. In the spectra [Eq. (4.6)] the only dependence on θ is through B disappearing for $\beta_{\text{in}} = 0$. It is also possible to restrict this dependence to such a term directly in Eqs. (3.2) and (3.3) by use of appropriate phase shifts of the modes. All of these operations account for

$$\begin{aligned} \frac{d\delta c}{d\tau} = -(1 + i\Delta)\delta c + \tilde{B}\delta c^\dagger + \sqrt{2\tilde{\gamma}_{nl}}\delta r_{\text{in}} \\ + \sqrt{2\tilde{\gamma}_c}\delta c_{\text{in}} + \sqrt{2\tilde{\gamma}_s}s_{\text{in}}, \end{aligned} \quad (5.1)$$

where the tilde represents division by γ_t , $\Delta = \tilde{\delta} + 2\tilde{\Gamma}n$, $\tilde{B} = 2\sqrt{\tilde{\mu}}\rho_{\text{in}} - (\tilde{\mu} + i\tilde{\Gamma})n$, and the modes are redefined as

$$c \equiv a \exp(-i\theta), \quad (5.2a)$$

$$c_{\text{in,out}} \equiv \frac{a_{\text{in,out}}}{\sqrt{\gamma_t}} \exp(-i\theta), \quad (5.2b)$$

$$r_{\text{in,out}} \equiv \frac{b_{\text{in,out}}}{\sqrt{\gamma_t}} \exp(-i2\theta), \quad (5.2c)$$

$$s_{\text{in}} \equiv \frac{w_{\text{in}}}{\sqrt{\gamma_t}} \exp(-i\theta). \quad (5.2d)$$

Consistent with the previous notation, ρ_{in} denotes the mean value of r_{in} . The boundary conditions of the new modes are

$$\delta c_{\text{out}} = \sqrt{2\tilde{\gamma}_c}\delta c - \delta c_{\text{in}}, \quad (5.3a)$$

$$\delta r_{\text{out}} = \sqrt{2\tilde{\gamma}_{nl}}\delta c - \delta r_{\text{in}}. \quad (5.3b)$$

For coherent states the correlations of the new input modes remain as white noise but in the scaled time τ . We shall refer to the previous formulas as the tilde normalization.

Quantum mechanical consistency, i.e., conservation of equal-time commutators, imposes a fluctuation-dissipation relation that under this normalization reads

$$\tilde{\gamma}_{nl} + \tilde{\gamma}_c + \tilde{\gamma}_s = 1. \quad (5.4)$$

The evolution equation (5.1), alongside with Eqs. (5.3), is now written in such a way that the input-output couplings are real valued as in the standard input-output formalism.^{28,29} In the case of a singly resonant system with $N - 1$ interacting waves, after the adequate normalization and phase shifts of the input modes, we have

$$\frac{d\delta c}{d\tau} = -(1 + i\Delta)\delta c + \tilde{B}\delta c^\dagger + \sum_{n=1}^N \sqrt{2\tilde{\gamma}_n}\delta c_{\text{in}}^n, \quad (5.5)$$

with

$$\sum_{n=1}^N \tilde{\gamma}_n = 1. \quad (5.6)$$

The frequency scale γ_t defining the dimensionless time τ is just the real part of the factor multiplying δc after the phase shifts. Here we assumed that there is no intracavity medium with population inversion. In such a case the corresponding gain is associated with a negative noise term proportional to the creation operator.

$N - 1$ of the input channels will have a time-reversed counterpart that corresponds to the outgoing modes, fulfilling

$$\delta c_{\text{out}}^n = \sqrt{2\tilde{\gamma}_n}\delta c - \delta c_{\text{in}}^n. \quad (5.7)$$

The remaining input is reserved to account for the irreversible losses. The physical picture that emerges from Eq. (5.5) envisages the stationary fluctuations of the intracavity mode as the (linear) response of the system to the noise introduced by the different inputs. Mathematically, the response is obtained by the convolution of the associated Green function (a 2×2 matrix), with the noise inputs. The intracavity mode itself disappears from the physical picture, and what matters is the action of the physical processes involved in the system dynamics (for instance, in the present case the two-photon absorption, the nonlinear phase shift, and the parametric amplification) onto the various inputs.

The corresponding output spectra are related to the intracavity spectra through

$$S_{-,+}^n(\tilde{\omega}) = 1 + : S_{-,+}^n(\tilde{\omega}) : = 1 + 2\tilde{\gamma}_n : S_{-,+}(\tilde{\omega}) :, \quad (5.8)$$

where $S_{-,+}(\tilde{\omega})$ is the intracavity spectra and $::$ denotes normal and time ordering; we have also used the proportionality of normally and time ordered intracavity and outgoing correlations.²⁹ The spectra $S_{-,+}^n(\tilde{\omega})$ coincide with the spectra of the original formulation as the new outgoing modes are just a phase shift of the originals.

Let us now define a sort of ideal reference system with only one input mode (time reversible), i.e.,

$$\frac{d\delta c}{d\tau} = -[1 + i\Delta]\delta c + \tilde{B}\delta c^\dagger + \sqrt{2}\delta c_{\text{in}}^{\text{ref}}, \quad (5.9)$$

$$\delta c_{\text{out}}^{\text{ref}} = \sqrt{2}\delta c - \delta c_{\text{in}}^{\text{ref}}. \quad (5.10)$$

For this reference system : $S_{-,+}^{\text{ref}}(\tilde{\omega}) = 2 : S_{-,+}(\tilde{\omega}) :$. As we are assuming independent input modes prepared in a coherent state, the cross correlations of their fluctuation operators are all zero while the self-correlations are all equal. In such a case and by virtue of Eq. (5.6), the intracavity spectra corresponding to Eqs. (5.5) and (5.9) are identical, so that we finally obtain

$$S_{-,+}^n(\tilde{\omega}) = 1 + \tilde{\gamma}_n : S_{-,+}^{\text{ref}}(\tilde{\omega}) :. \quad (5.11)$$

This is the central result of this section. Let us elaborate a little about its interpretation. Squeezing in a given output mode means that for a certain range of the phase, the corresponding quadratures show an intensity of its fluctuations below that of the associated incoming mode (assumed in a coherent state). In view of Eq. (5.7), the amplitude of the outgoing fluctuations is a coherent superposition of the intracavity and the incoming fluctuations. Squeezing is possible if an adequate correlation between δc and the relevant input fluctuation operator is established. But δc is given by the response of the intracavity system to the noise inputs. The input modes are uncorrelated and so is the dynamic response to them. A given input mode can consequently correlate only with the dynamic response to itself. The presence of any other noise input can only degrade the effect. The great advantage of the tilde normalization is that it makes this fact explicit. Indeed, Eq. (5.11) expresses the output spectra as the dynamic response of the system to an isolated input mode, i.e., : $S_{-,+}^{\text{ref}}(\tilde{\omega}) :$, scaled down by the static contribution to the accumulated noise owing to the presence of extra input modes. The scale factor $\tilde{\gamma}_n$ is just the ratio between the input–output coupling constant of the chosen mode and the sum of all of them. As an immediate consequence, the squeezing is limited to

$$S_M^n = 1 - \tilde{\gamma}_n, \quad (5.12)$$

a bound that cannot be surpassed whatever the dynamic response of the system.

Equation (5.11) greatly simplifies our task of finding the optimum paths to maximum noise reduction, since we can focus our efforts on the simple reference system described by Eqs. (5.9) and (5.10). The normally ordered spectra of the reference system are

$$\begin{aligned} & : S_{-,+}^{\text{ref}}(\tilde{\omega}) : \\ & = 4|\tilde{B}| \frac{2|\tilde{B}| \mp \sqrt{(1 + \tilde{\omega}^2 + |\tilde{B}|^2 - \Delta^2)^2 + 4\Delta^2}}{(1 - \tilde{\omega}^2 - |\tilde{B}|^2 + \Delta^2)^2 + 4\tilde{\omega}^2}. \end{aligned} \quad (5.13)$$

Our first step is to determine if the dynamic response is capable of total noise suppression. Perfect squeezing can occur only at a dynamic instability. After equating the left-hand side of Eq. (3.10) (the only possible unstable eigenvalue) to zero and after proper normalization, we can write an equation that determines the instability as

$$1 + \Delta^2 = |\tilde{B}|^2. \quad (5.14)$$

Insertion of the instability condition in : $S_{-,+}^{\text{ref}}(\tilde{\omega}) :$ results in

$$: S_{-,+}^{\text{ref}}(\tilde{\omega}) : = 4|\tilde{B}| \frac{2|\tilde{B}| - \sqrt{4|\tilde{B}|^2 + \tilde{\omega}^2(\tilde{\omega}^2 + 4)}}{\tilde{\omega}^2(\tilde{\omega}^2 + 4)}. \quad (5.15)$$

The application of L'Hôpital's rule with respect to $\tilde{\omega}^2$, : $S_{-,+}^{\text{ref}}(\tilde{\omega}) :$ equals -1 at $\tilde{\omega} = 0$; that is, perfect squeezing is obtained at the instability. In other words, the dynamic response of the system, assuming that condition (5.14) is reachable, is capable of a complete suppression of quantum noise.

Spectrum [Eq. (5.13)] is simple enough to permit analytic optimization. Taking partial derivative in : $S_{-,+}^{\text{ref}}(\tilde{\omega}) :$ with respect to $\tilde{\omega}$ and equaling to zero, $\tilde{\omega} = 0$ appears as the optimum point, whatever the values of Δ and $|\tilde{B}|$ are. The same applies to $\Delta = 0$ when we take partial derivative with respect to Δ . Δ is the detuning of the linearized evolution, and thus what we have obtained is that the best working point is at resonance. The optimized spectra obtained imposing these two conditions simplifies to

$$: S_{-,+}^{\text{opt}} : = \mp \frac{4|\tilde{B}|}{(1 \pm |\tilde{B}|)^2}. \quad (5.16)$$

: $S_{-,+}^{\text{opt}}$: shows a minimum at the instability $|\tilde{B}| = 1$, which is approached monotonically. These conditions ($\tilde{\omega} = 0$, $\Delta = 0$, and $|\tilde{B}| = 1$) will help us in finding optimum paths. In particular, by moving $|\tilde{B}|$ from zero to one while maintaining $\Delta = \tilde{\omega} = 0$ we can define the optimum path that reaches the instability for the reference model with the minimum and maximum noise along it given by Eq. (5.16). For any finite n , $\Delta \equiv \tilde{\delta} + 2n\tilde{\Gamma} = 0$ implies $\tilde{\delta} + 2n\tilde{\Gamma} = 0$, and, as explained at the end of Section 4, the phase of the most squeezed quadrature is then independent of the frequency. In any specific implementation of the system, Δ and $|\tilde{B}|$ will depend in general on several parameters. Note that once $|\tilde{B}| = 1$ is reached, any path belonging to the manifold defined by Eq. (5.14) will be optimum but unstable.

An optimum path is defined solely by the squeezing spectrum, leaving aside the stretching one. It is also important to study the accompanying excess noise on the conjugate quadrature, since it could invalidate in practice the optimum path if this excess noise is unbearably high. The minimal excess noise production imposed by the Heisenberg principle corresponds to $S_{-}(\omega)S_{+}(\omega) = 1$. Adding 1 to Eq. (5.13) and after some minor algebra, we obtain

$$S_{-,+}^{\text{ref}}(\tilde{\omega}) = \frac{[2|\tilde{B}| \pm \sqrt{(\tilde{\omega}^2 + |\tilde{B}|^2 + 1 - \Delta^2)^2 + 4\Delta^2}]^2}{(1 - \tilde{\omega}^2 - |\tilde{B}|^2 + \Delta^2)^2 + 4\tilde{\omega}^2}. \quad (5.17)$$

Straightforward algebra leads to $S_{-}^{\text{ref}}(\tilde{\omega})S_{+}^{\text{ref}}(\tilde{\omega}) = 1$, and thus the excess noise is minimum.

B. Standard Normalization

As discussed in the Introduction, we are here principally interested in the squeezing behavior with respect to the

photon number n . The tilde normalization will be very useful to optimize the performance but is inappropriate to study the dependence on n . It is far more convenient to use γ^{-1} as the time scale instead of γ_t^{-1} and to normalize the photon number as $m = \nu n/\gamma$. In complete parallelism to the tilde normalization, we have then

$$\begin{aligned} \frac{d\delta c}{d\tau} = & -[1 + 2mK_r + i(\hat{\delta} + 2mK_i)]\delta c \\ & + [\sqrt{K_r}\eta_{\text{in}} - (K_r + iK_i)m]\delta c^\dagger + 2\sqrt{mK_r}\delta r_{\text{in}} \\ & + \sqrt{2\hat{\gamma}_c}\delta c_{\text{in}} + \sqrt{2\hat{\gamma}_s}s_{\text{in}}, \end{aligned} \quad (5.18)$$

where the hat represents division by γ and

$$\eta_{\text{in}} \equiv \frac{2\sqrt{\nu}}{\gamma}\beta_{\text{in}}\exp(-i2\theta), \quad (5.19)$$

which represents the harmonic mode input amplitude normalized to the value at the standard OPO threshold. The spectra in this normalization are obtained from the following translations in Eqs. (4.6) and (4.7): $\gamma \rightarrow 1$, $n \rightarrow m$, $\mu \rightarrow K_r$, and $\Gamma \rightarrow K_i$. A hat should also be placed over ω , γ_c , γ_s , δ , and B . In the hat normalization, \hat{B} reduces to $\sqrt{K_r}\eta_{\text{in}} - (K_r + iK_i)m$. Note the different characters of the tilde and the hat normalizations. The former is thought to lead to clearer physical insight by considering the linearized evolution equations as corresponding to a hypothetical linear system where n is constant. The time scale is chosen as the inverse of the losses of the linear system, so that the nonlinearity is hidden in the normalization constant. On the other hand, the hat normalization makes a closer contact with the real experiment by considering the ratio between the nonlinearity and the losses (ν/γ) as the relevant figure of merit rather than the nonlinearity itself.

Given the above translation table, $K_i(\Delta k)$ is identified as an effective Kerr-effect constant (caused by the cascading effect) and $K_r(\Delta k)$ is identified as the equivalent for two-photon absorption (caused by the upconversion of photons to a nonresonant mode). Through its square root, $K_r(\Delta k)$ also plays the role of an effective downconversion constant.

Some care must be taken when the quantum noise behavior is studied as a function of n (or m). This is not a free parameter as the amplitude of the input modes or the phase mismatch would be, but it is in a nonlinear relation with them. We need, therefore, to check that the proposed values of n are indeed a solution of Eq. (3.7). Fortunately, the spectra [Eq. (4.6)] do not depend on the overall sign of $\delta + 2\Gamma n$, and therefore the conclusions reached in Section 3 regarding the existence of $|\alpha_{\text{in}}|$ permit a safe variation of n in search of strong noise reduction, provided that the corresponding fixed points are stable.

C. Squeezing at the Fundamental Mode

Applying Eq. (5.11) to the fundamental mode, we obtain

$$S_{-,+}^a(\tilde{\omega}) = 1 + \tilde{\gamma}_c : S_{-,+}^{\text{ref}}(\tilde{\omega}) :. \quad (5.20)$$

The static limit [Eq. (5.12)] is in this case

$$S_M^a = 1 - \tilde{\gamma}_c = \frac{\gamma_s + 2\mu n}{\gamma_s + \gamma_c + 2\mu n} = \frac{\hat{\gamma}_s + 2K_r(\Delta k)m}{1 + 2K_r(\Delta k)m}. \quad (5.21)$$

The best static performance corresponds to $\gamma_{nl} = 2\mu n = 0$, that is, either $n = 0$ or $\mu = 0$. In this case $\tilde{\gamma}_c$ maximizes to $\hat{\gamma}_c = \gamma_c/(\gamma_c + \gamma_s)$. The parameter $\hat{\gamma}_c$ is known as the escape efficiency of the cavity. The case $n = 0$ corresponds to the well-known case of squeezed vacuum generation (an OPO below threshold). The first value of the phase mismatch for which $\mu = \nu K_r(\Delta k) = 0$ is $\Delta k L_m = 2\pi$ (see Fig. 1). The system is then formally equivalent to a resonant optical Kerr-effect system whose quantum noise behavior has been amply studied previously.³⁰ The condition (5.14) for $\mu = 0$ implies detunings fulfilling $\delta_{\pm} = -2n\Gamma \pm (n^2\Gamma^2 - \gamma^2)^{1/2}$, the well-known turning points of optical dispersive bistability. Such cascading-induced bistability has been experimentally demonstrated in Ref. 25. With $\Delta k L_m = 2\pi$, $K_i(2\pi) = 1/\pi$ and $|\tilde{B}|$ reduces to m/π . Substituting into Eq. (5.16),

$$: S_{-,+}^{\text{opt}} : = \mp \frac{4m\pi}{(\pi \pm m)^2}. \quad (5.22)$$

The associated squeezing and stretching spectra are given by

$$S_{-,+}^a(0) = 1 \mp \hat{\gamma}_c \frac{4m\pi}{(\pi \pm m)^2}. \quad (5.23)$$

Below $m = \pi$ there is only one optimum path that reaches the instability: to vary m from zero to π while maintaining $\omega = \Delta = 0$. Translating to the original variables and taking into account that the phase mismatch is fixed to 2π , we can define the optimum path by the constraint $\delta + 2\Gamma n = \delta + 2\nu n/\pi = 0$. Figure 2 displays the behavior of $S_{-,+}^a(0)$ along this optimum path for three values of the escape efficiency, 0.9, 0.99 and the ideal 1. The noise is expressed in dB's with respect to the vacuum noise. Heisenberg-limited excess noise appears in such a case as a specular image of the squeezing with respect to the zero dB's line. The instability is signaled by the divergence in the excess noise. This shows excel-

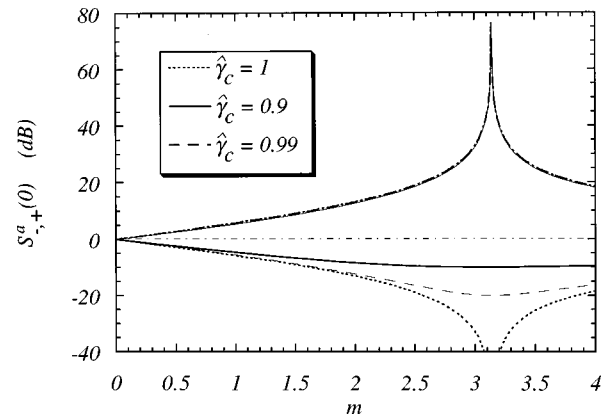


Fig. 2. Noise spectra at zero frequency of the fundamental mode following an optimum path for three escape efficiencies of the cavity, including the ideal case $\hat{\gamma}_c = 1$. The curves above the divergences are not physical.

lent behavior in the sense that its deleterious influence has a very short range. When the excess noise falls below 30 dB (nothing dramatic if compared with the typical technical noise of a laser), the squeezing is almost at maximum in the $\hat{\gamma}_c = 0.9$ case and only slightly below maximum when $\hat{\gamma}_c$ equals 0.99. This latter case also shows Heisenberg-limited excess noise through most of the optimum path. This good behavior can be expected for all singly resonant devices of the kind represented by Eqs. (5.5) and (5.7), since the reference system shows Heisenberg-limited quantum noise. Above the divergence, the curves shown are not physical, since they correspond to unstable fixed points.

Where $\mu = 0$, the formulas simplify enough to allow a simple expression for the squeezing phase. As $\Delta = 0$ implies $\delta + 2\Gamma n = 0$, ϕ_{opt} is determined by B . More specifically, $B = -i\Gamma\alpha^2$ gives $\phi_{\text{opt}} = \theta + \pi/2$. On the other hand, substituting Eq. (3.5) into Eq. (2.5a) results in $\sqrt{2}\gamma_c\alpha_{\text{out}} = \alpha(\gamma_c - \gamma_s + i\Gamma n)$, giving a squeezing phase relative to that of the output field of

$$\frac{\pi}{2} - \arctan\left(\frac{\Gamma n}{\gamma_c - \gamma_s}\right).$$

At the instability $\Gamma n = \gamma$, and for low γ_s ($\hat{\gamma}_c \approx 1$) it approaches $\pi/4$.

D. Squeezing at the Harmonic Mode

For the harmonic mode Eq. (5.11) yields

$$S_{-,+}^b(\tilde{\omega}) = 1 + \tilde{\gamma}_{nl} : S_{-,+}^{\text{ref}}(\tilde{\omega}) :, \quad (5.24)$$

with a static limit

$$S_M^b = 1 - \tilde{\gamma}_{nl} = \frac{\gamma}{\gamma + 2\mu n} = \frac{1}{1 + 2K_r(\Delta k)m}. \quad (5.25)$$

Now the situation is the complete opposite: Performance is favored by a finite μ and a large n . In fact, under ideal conditions of perfect dynamic noise suppression and no absorption and scattering losses ($\gamma_s = 0$), the squeezing in both modes is complementary in the sense of

$$\begin{aligned} S_-^a(0) + S_-^b(0) &= 2 - \tilde{\gamma}_c - \tilde{\gamma}_{nl} \\ &= 2 - \frac{\gamma_c}{\gamma + 2\mu n} - \frac{2\mu n}{\gamma + 2\mu n} = 1, \end{aligned} \quad (5.26)$$

a direct consequence of the fluctuation–dissipation relation [Eq. (5.6)]. This complementarity has been previously reported for the doubly resonant degenerate parametric oscillator.³¹

The static limit of noise reduction is now nonlinear in the sense that it depends on the phase mismatch and m . An immediate consequence of Eq. (5.25) is the possibility of an arbitrarily large quantum noise reduction for any finite value of $K_r(\Delta k)$. The 1/9 limit of the conventional phase-matched SHG is therefore due to a failure of the setup to maximize the dynamic response of the system as far as quantum noise reduction is concerned. Let us first focus on the SHG-like case ($\beta_{\text{in}} = 0$). The instability points are now given by (directly in the hat normalization)

$$\begin{aligned} \hat{\delta}_{\pm} &= -2mK_i(\Delta k) \\ &\pm \sqrt{m^2[K_i(\Delta k)^2 - 3K_r(\Delta k)^2] - 4K_r(\Delta k)m - 1}. \end{aligned} \quad (5.27)$$

Both kinds of nonlinearities (dispersive and absorptive) are in this case necessary, since the factor $K_i(\Delta k)^2 - 3K_r(\Delta k)^2$ needs to be positive to allow $\hat{\delta}_{\pm}$ to be real. The phase-matched case is therefore excluded. A numerical evaluation of $K_i(\Delta k)^2 - 3K_r(\Delta k)^2$ shows that just above $\Delta k = \pi$ it becomes positive. This is a remarkable result, since the phase mismatch diminishes the effective interaction between the modes. In spite of this, far from having a deleterious effect, it allows for arbitrarily large degrees of squeezing. This counterintuitive effect can be understood as follows. In the phase-matched case the only physical process present is the two-photon absorption. But it is of limited efficiency, since its absorptive nature implies an associated input noise, so that the squeezing saturates to the 1/9 value. On the other hand, the dispersive nonlinearity is a Hamiltonian process with no associated input noise, so that it can yield perfect squeezing at the ideal limit. A finite phase mismatch switches on the nonlinear phase shift. When adequate parameters are chosen, both processes collaborate to reduce the vacuum noise. In spite of the lower effective interaction, the system profits from the high efficiency of the nonlinear phase shift, leading in the optimum case to arbitrarily large squeezing. Note, however, that the lower effective interaction implies a rising of the static limit [Eq. (5.25)], which is minimum for the phase-matched case.

Optimum approaches to the instability [Eq. (5.27)] are more difficult to evaluate than in the fundamental mode, since the static limit now also depends on m and Δk . With respect to m , it is clear that the static part is optimized at $m \rightarrow \infty$. This limit can be approached by letting $\tilde{\omega} = 0$ and $\hat{\delta} = -2K_i(\Delta k)m$ (i.e., $\Delta = 0$). $|\tilde{B}|$ reduces in this case ($\beta_{\text{in}} = 0$) to $m(K_r(\Delta k)^2 + K_i(\Delta k)^2)^{1/2}/[1 + 2mK_r(\Delta k)]$, showing a monotonic increasing behavior with respect to m from 0 to the maximum (at $m \rightarrow \infty$):

$$|\tilde{B}| = \frac{1}{2} \left\{ 1 + \left[\frac{K_i(\Delta k)}{K_r(\Delta k)} \right]^2 \right\}^{1/2}. \quad (5.28)$$

Note that for $K_i(\Delta k)^2 = 3K_r(\Delta k)^2$, $|\tilde{B}|$ consistently equals 1. We have then both $\tilde{\gamma}_{nl} = 1$ and the fastest approach to 1 of $|\tilde{B}|$ when $m \rightarrow \infty$. Therefore squeezing along an optimum path with respect to Δk is given by substituting Eq. (5.28) in the spectrum [Eq. (5.16)] and then substituting the obtained $S_{\text{opt}}^{\text{ref}}$ into Eq. (5.24). In a real experiment m can be large but finite. To be specific, let us take as a large m one giving a static limit S_M^b of ~ 20 dB. This corresponds to $m = 50$. Figure 3 displays $S_{-,+}^b(0)$ as a function of the phase mismatch in such a case. To illustrate the modulation exerted by S_M^b , this time we made $\hat{\delta}$ equal to the real part of Eq. (5.27) plus a very small number. In this way the plot remains valid for the whole range of $\Delta k L_m$. Where Eq. (5.27) is complex, the condition $\Delta = 0$ is almost fulfilled. Above the instability, noise-suppression reduction follows S_M^b .

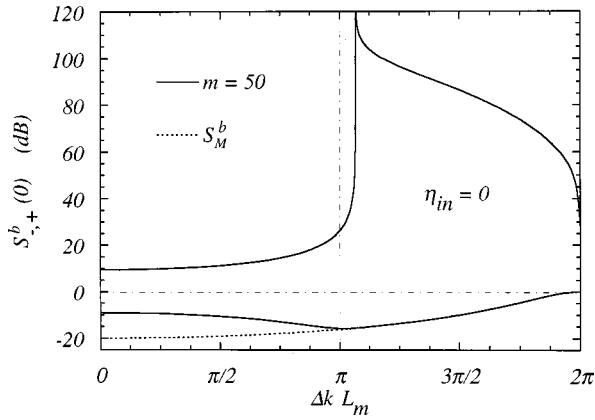


Fig. 3. Noise spectra at zero frequency of the harmonic mode following a nearly optimum path with respect to the phase mismatch for the SHG-like case.

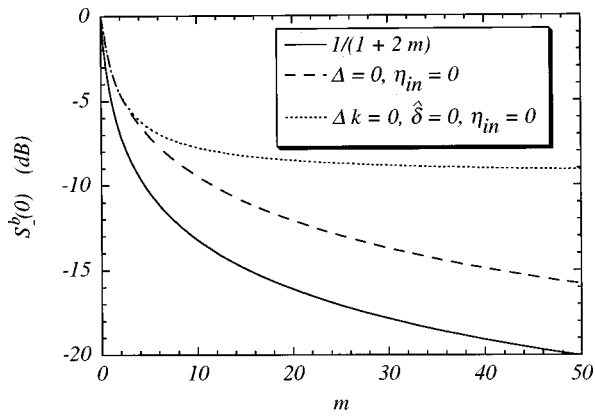


Fig. 4. Squeezing in the harmonic mode along an optimum path with respect to the normalized intracavity photon number (m) for the SHG-like case, compared with the phase-matched SHG case and the minimum static limit.

Again, the pernicious effect of the instability regarding the excess noise has a very short range.

The optimum path with respect to m is much more complicated to find because of the intricate dependence of $K_i(\Delta k)$ and $K_r(\Delta k)$ with respect to the phase mismatch. The dashed curve of Fig. 4 has been found by numerically locating the minima of $S_{-,+}^b(0)$ with respect to m . As a comparison, the phase-matched static limit (solid curve) and SHG (dotted curve) are also depicted. For low values of m the instability [Eq. (5.27)] is not accessible and the optimum path corresponds to maximize $\tilde{\gamma}_{nl}$, i.e., $K_r(0) = 1$, the phase-matched case. As soon as the instability is accessible, the two curves depart from each other and the optimum path becomes unstable and should then be taken as a mathematical limit. However, in view of Fig. 3, again, bearable values of the excess noise are possible with only a slight diminution of the squeezing.

It is worth mentioning that a squeezing as large as 48% induced by cascading has been recently reported.³² The cascading was due, however, to a detuning of the pump mode in a triply resonant nondegenerate OPO with a much lower finesse for the pump mode rather than by phase mismatch. Under such conditions, a cascaded $\chi^{(3)}$ is also induced that can lead in the linear approximation to perfect squeezing in the pump mode.

Alternatively to the nonlinear phase shift induced by cascading, we can use the parametric amplification that emerges when $\beta_{in} \neq 0$. This process is maximized for phase-matched interactions and therefore does not suffer from an overall diminution of efficiency. To take advantage of a collaboration between the two-photon absorption and the parametric amplification, it is necessary to fulfill Eq. (5.14) at $\Delta k = 0$. Constructing an optimum path with respect to the new parameter η_{in} is just a matter of imposing $\Delta = \tilde{\omega} = 0$, since the static limit [Eq. (5.25)] does not depend on it. As the nonlinear phase shift vanishes [$K_i(0) = 0$], $\Delta = 0$ is equivalent to $\hat{\delta} = 0$. It is easy to check that $|\tilde{B}|$ equals $|\eta_{in} - m|/(1 + 2m)$. Therefore, through an optimum path, the instability condition (5.14) simplifies to

$$1 + 2m = |\eta_{in} - m|, \quad (5.29)$$

a perfectly achievable condition. From Eqs. (5.16) and (5.25) we have for the noise along the optimum path

$$S_{-,+}^b(0) = \left(\frac{1 + 2m \mp |\eta_{in} - m|}{1 + 2m \pm |\eta_{in} - m|} \right)^2. \quad (5.30)$$

We can further optimize by choosing an adequate phase of η_{in} so that \tilde{B} approaches 1 as much as possible. The extreme cases correspond to η_{in} real; i.e., $\eta_{in} = -(1 + m)$ and $\eta_{in} = 1 + 3m$. From Eqs. (3.8) and (3.9) it is easy to check that they correspond to $\theta_{in} - \varphi_{in}/2 = \pi$ and $\theta_{in} - \varphi_{in}/2 = 0$, respectively. The negative case maximizes $|\tilde{B}|$. It has been previously reported in Ref. 27. Taking the square modulus of Eq. (2.5b), we see that the negative case appears to promote harmonic output power while the converse is true for the positive. The squeezing phase is also easy to calculate in this case. In particular, given the correlation [Eq. (4.8b)], $\epsilon(\omega)$ is determined by the phase of $\alpha^2 B$ (independent of ω as $\Delta = 0$). The corresponding squeezing phases are $\phi_{opt} = 2\theta + \pi$ for the negative case. For the positive case it changes from $\phi_{opt} = 2\theta + \pi$ to $\phi_{opt} = 2\theta + \pi/2$ at $\eta_{in} = m$. On the other hand, the output harmonic amplitude is proportional to [see Eq. (2.5b)]

$$b_{out} \propto (\eta_{in} - 2m) \exp[i(2\theta + \pi)]. \quad (5.31)$$

Therefore the relative squeezing phase for the negative η_{in} is π , i.e., amplitude squeezing. The positive case is more complicated. It remains equal to π (amplitude squeezing) until $\eta_{in} = m$. Above this value it changes to $\pm \pi/2$, depending on the sign of $\eta_{in}/2 - m$, yielding, in any case, phase squeezing. At a first glance, it appears that there is a sudden change from amplitude to phase squeezing when the input phases are set to $\theta_{in} - \varphi_{in}/2 = 0$ and $|\eta_{in}|$ passes through m . It is not so, however, since at this point $B = 0$, and the state collapses to a coherent state with no squeezing. The situation is clearly illustrated in Fig. 5, where $S_{-,+}^b(0)$ are displayed as a function of η_{in} assumed real. The right-hand side of the plot corresponds to $\theta_{in} - \varphi_{in}/2 = 0$; left-hand side corresponds to $\theta_{in} - \varphi_{in}/2 = \pi$. The negative ordinates correspond to follow an optimum path with respect to η_{in} . The behavior is completely symmetric with respect to $\eta_{in} = m$, where both the squeezing and the excess noise equal those of the vacuum.

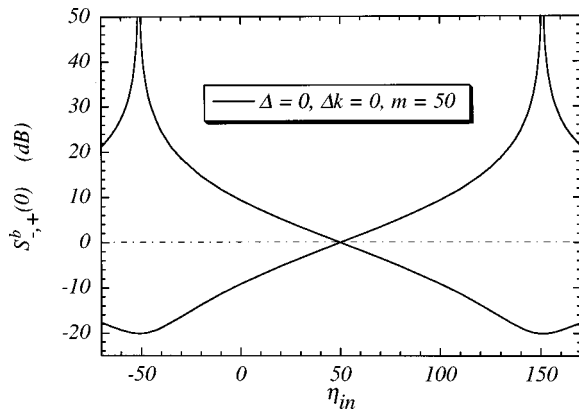


Fig. 5. Noise spectra at zero frequency (harmonic mode) following an optimum path with respect to the normalized input harmonic amplitude (η_{in}). The curves are not physical above the divergences.

The optimum path with respect to m is now given by S_M^b at $K_r(0) = 1$, i.e., $1/(1 + 2m)$, and is depicted in Fig. 4 with a solid curve. It represents the maximum efficiency the system can yield as far as quantum noise reduction in the harmonic mode is concerned with respect to m . This maximum efficiency happens when the coupling between the two waves is maximum and the parameters are such that the two-photon absorption and the parametric amplification optimally collaborate in the squeezing process. The improvement with respect to the standard phase-matched SHG as well as to the optimized SHG is considerable. Obviously, this is an unstable path, but once again, in view of the excellent behavior of the divergences in Fig. 5 for η_{in} within bearable values of the excess noise, the squeezing should not depart substantially from S_M^b . Indeed, this is the case as it is illustrated in Section 6.

6. DISCUSSION AND CONCLUSIONS

The present paper has two main purposes: first, to gain physical insight about the origins of quantum noise in singly resonant systems and second, to explore their potential as squeezed light sources. For such an endeavour we used a workable model that includes all the relevant physics we want to address. The results shown in the previous sections certainly reveal a high potential for the studied configurations. An evaluation of the limits of the model in reproducing the real physical situation, as well as a discussion of possible implementations, seems therefore in order.

One obvious idealization of the model is to assume perfectly coherent inputs, neglecting the excess noise of real lasers (something expected to have deleterious effects at low frequencies). White *et al.*³³ have developed an analytical approach to this problem, which resulted in an impressive agreement with experiments. As expected, the excess noise completely destroys the squeezing at low frequencies. In their experiments, however, the deleterious effect was restricted to only 7 MHz by adding a mode cleaner to the system, the spectrum coinciding with the ideal one out of this range. Even better, in Ref. 11 the

laser noise was shot-noise limited down to 1 MHz, again with an external mode cleaner.

Assuming coherent states for the input modes as well as a value of $m \sim 3$ (we will see below it looks like the case), our main concern about the fundamental mode results that are summarized in Fig. 2 refers to the feasibility of the chosen escape efficiencies. The ratio $\gamma_c/(\gamma_c + \gamma_s)$ is difficult to maximize in a resonant mode because, by its very nature, γ_c must be rather low. Thus in Ref. 25 it was only of 0.52, while in Ref. 4 it was 0.36. Even in Ref. 3, a doubly resonant system specifically designed to squeeze the fundamental mode, the escape efficiency was ~ 0.9 , limiting the maximum squeezing achievable to 90% (in practice, a 52% of noise reduction was reached). It appears, then, that nowadays the $\hat{\gamma}_c = 0.99$ case should be taken rather as an ideal illustrative case.

In contrast, the ultimate limit for noise suppression in the harmonic mode [Eq. (5.25)] is pushed up by the fundamental mode photon number, clearing a way to bypass the limit imposed by the escape efficiency of the cavity, which cannot be modified once the device is built. Therefore the squeezing in the harmonic mode can be arbitrarily large under the ideal assumption that the energy load inside the cavity can also be arbitrarily large. However, this is not totally true, as the model does not take into account the losses in the harmonic mode that necessarily limit the degree of noise suppression. We can estimate this limitation, assuming that the absorption in one single pass through the nonlinear material is equivalent to the effect of a beam splitter with adequate reflectivity. Taking an absorption of 0.6%/cm as in Ref. 3 and a length of 1 cm, the equivalent reflectivity would be of 6×10^{-3} . The spectrum after the beam splitter is given by $S_{out} = 1 + T: S_{in}:$. Setting $: S_{in}: = -1$ and $T = 1 - R$, the ultimate squeezing achievable is precisely $R = 6 \times 10^{-3}$, i.e., -22 dB. In other words, the chosen value of $m = 50$ in Figs. 3 and 5 is approximately the maximum that the model can stand without the inclusion of the harmonic mode losses.

Of course, we still cannot assume $m = 50$ as a realistic limit for the state of the art devices, since m depends not only on the intracavity photon number but also on the ratio ν/γ between the nonlinearity and losses. This ratio must be high enough to prevent a degradation of the nonlinear optical response of the system, as noted in the Introduction. Besides, this ratio scales down the power available in the external sources. In view of these complications, probably the most reliable way of setting the physical scale of m is to compare the results with the reported experiments. In Ref. 6 the quoted noise reduction was -5.2 dB. Setting Δk to zero and having β_{in} correspond to phase-matched SHG as reported, we find that a -5.2 dB squeezing results at $m = 2.5$, far from the $m = 50$ limit. Fortunately, the limit [Eq. (5.25)] grows up quite quickly for low m 's (see Fig. 4). Thus 10 dB of noise suppression are reached for $m = 5$, which is a reasonable value. However, -15 dB of noise reduction requires $m = 15$, while a -20-dB figure is at the $m = 50$ limit. New nonlinear materials seem to be the only possibility for such high squeezing degrees. A promising method consists in the use of resonant nonlinearities in asymmet-

ric quantum wells. Huge nonlinearities, and even a tuning of the nonlinearity with a dc field,³⁴ have been demonstrated in frequency-doubling experiments. Obviously, the absorption is also enhanced by the resonance. This can be a problem, as the ratio ν/γ could not be increased at the end of the day. We can foresee, however, a promising advantage in that the losses in the harmonic mode have little influence on performance. By the maintenance of a strong two-photon resonance but by the relaxation of the one-photon counterpart (tuning with a dc field or by adequate energy-level engineering), the nonlinearity would certainly be enhanced while the losses at the fundamental mode would not increase so strongly, thus enhancing ν/γ . With only one passage through the cavity of the harmonic mode, and taking into account that a very thin layer of material is capable of SHG,³⁴ the associated deleterious effect cannot be very large. An even more exciting possibility comes from the recent experimental demonstrations of absorption inhibition in asymmetric quantum wells induced by quantum interference.³⁵⁻³⁷ The absorption inhibition and the resonant enhancement can be combined by use of quantum well engineering, resulting in very efficient frequency doublers (see Ref. 38, where such a scheme that is resonant only at the harmonic mode is proposed).

These are promising perspectives, but we should not dismiss the improvements linked to the performances of the present nonlinear crystals. Let us focus on $m = 2.5$. As shown in Section 5, the best strategy corresponds to drive both modes with the relative phases $\varphi_{in} - \theta_{in}/2 = \pi/2$ (negative η_{in}) and $\Delta = 0$. In Fig. 6 noise behavior is displayed for various distances to the instability [Eq. (5.29)]. Even at half the instability η_{in} value, the squeezing at $m = 2.5$ grows from -5.1 dB (69%) to -7.2 dB (80%). The excess noise, on the other hand, rapidly increases at low m 's, but it also saturates quickly to bearable values. Although there are no abrupt changes, the improvement is quite substantial. This was not acknowledged in Ref. 27, in which noise suppression was studied as function of the input power. Given its nonlinear relation with m , the improvement is much slower with respect to this variable. Besides the squeezing, the output

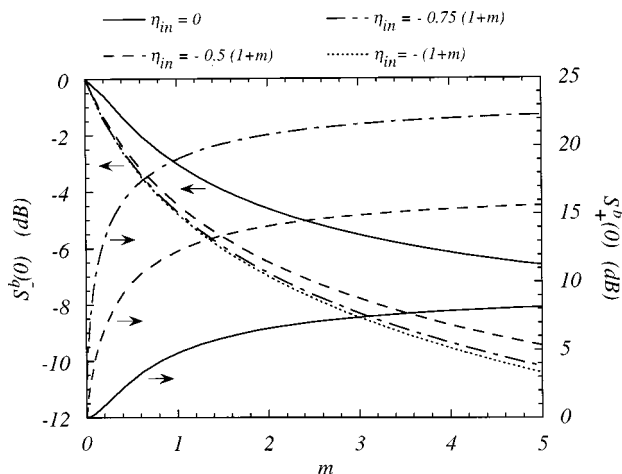


Fig. 6. Noise spectra at zero frequency (harmonic mode) for $\Delta k = \delta = 0$ as function of the normalized intracavity photon number at various distances from the dynamic instability.

power is also enhanced. When a negative η_{in} is used in Eq. (5.31), the output power results in $P_{out} \propto (2m + |\eta_{in}|)^2$, and thus the harmonic mode input contributes constructively to it. A numerical inspection shows how even at half the way to the instability the power is nearly doubled. Although from the theoretical point of view the injection of a coherent signal in the harmonic mode looks quite harmless, the experimental implementation is not trivial. However, the remarkable achievements in Refs. 10 and 11 with the optical parametric amplification strongly support the feasibility of the idea.

Finally, a word of caution about the design of the device. It is important to avoid setting oscillations out of the fundamental mode (the so-called subharmonic pumped OPO,^{39,40} also known as internally pumped OPO⁴¹), since this is capable of destroying the noise reduction.⁴² At a first glance, finite values of η_{in} appears to favor the effect by promoting the downconversion. But downconversion is enhanced only for a given range of the relative phase between the two driving fields. Thus, for the negative η_{in} case studied above, when the harmonic output power is maximized, the downconversion is minimized.

To conclude, let us summarize the most relevant results. First, for a class of systems that is useful for squeezing generation we have presented a systematic approach capable of disentangling in the spectra the dynamic response of the system out of the contribution coming from the various noisy inputs. We have also presented the conditions that optimize the dynamic response with respect to the squeezing effect. The procedure has been applied to the case of a singly resonant second-order nonlinear device with the following results. The squeezing at the fundamental mode is ultimately limited by the escape efficiency of the cavity, the best working point being within figures of merit of conventional nonlinear crystals. With respect to the harmonic mode, the $1/9$ squeezing limit present in the standard phase-matched case is due to a nonoptimum dynamic response. A finite phase mismatch or a driving in the harmonic mode allow for a complete optimization, leading to a squeezing ultimately limited by the losses of the harmonic mode. The fact that noise reduction is limited only by the losses in the nonresonant mode opens the possibility of the use of resonantly enhanced nonlinearities that would yield very high squeezing. At any rate, the use of standard nonlinear crystals may possibly provide a substantial improvement with respect to the reported experiments by injecting a coherent driving field in the harmonic mode. In addition, the output power would be highly enhanced.

ACKNOWLEDGMENTS

C. Cabrillo thanks S. Schiller and especially A. G. White for useful comments and suggestions. The paper was supported in part by grants TIC95-0563-C05-03 and PB96-00819 from Comisi3n Interministerial de Ciencia y Tecnolog3a, Spain and Comunidad de Madrid 06T/039/96, Spain.

*Present address, Instituto de Optica, Serrano 121, 28006, Madrid, Spain. The author can also be reached by e-mail at ccabrillo@foton0.iem.csic.es.

REFERENCES

1. S. F. Pereira, X. Min, H. J. Kimble, and J. L. Hall, "Generation of squeezed light by intracavity frequency doubling," *Phys. Rev. A* **38**, 4931–4934 (1988).
2. A. Sizmann, R. J. Horowicz, and G. Wagner, "Observation of amplitude squeezing of the up-converted mode in second harmonic generation," *Opt. Commun.* **80**, 138–142 (1990).
3. P. Kurz, R. Paschotta, K. Fiedler, and J. Mlynek, "Bright squeezed light by second-harmonic generation in a monolithic resonator," *Europhys. Lett.* **24**, 449–454 (1993).
4. R. Paschotta, M. Collett, and P. Kurz, "Bright squeezed light from a singly resonant frequency doubler," *Phys. Rev. Lett.* **72**, 3807–3810 (1994).
5. T. C. Ralph, M. S. Taubman, A. G. White, D. E. McClelland, and H.-A. Bachor, "Squeezed light from second-harmonic generation: experiment versus theory," *Opt. Lett.* **20**, 1316–1318 (1995).
6. H. Tsuchida, "Generation of amplitude squeezed light at 431 nm from a singly resonant frequency doubler," *Opt. Lett.* **20**, 2240–2242 (1995).
7. S. Youn, S.-K. Choi, P. Kumar, and R.-D. Li, "Observation of sub-Poissonian light in traveling-wave second-harmonic generation," *Opt. Lett.* **21**, 1597–1599 (1996).
8. E. S. Polzik, J. Carri, and H. J. Kimble, "Atomic spectroscopy with squeezed light for sensitivity beyond the vacuum state limit," *Appl. Phys. B* **55**, 279–290 (1992).
9. G. Breitenbach, T. Müller, S. F. Pereira, J.-Ph. Poizat, S. Schiller, and J. Mlynek, "Squeezed vacuum from a monolithic optical parametric oscillator," *J. Opt. Soc. Am. B* **12**, 2304–2309 (1995).
10. K. Schneider, R. Bruckmeier, H. Hansen, S. Schiller, and J. Mlynek, "Bright squeezed-light generation by a continuous-wave semimonolithic parametric amplifier," *Opt. Lett.* **21**, 1396–1398 (1996).
11. G. Breitenbach, S. Schiller, and J. Mlynek, "Measurement of the quantum states of squeezed light," *Nature* **387**, 471–475 (1997).
12. K. Sundar, "Highly amplitude squeezed states of the radiation field," *Phys. Rev. Lett.* **75**, 2116–2119 (1995).
13. M. A. M. Marte, "Sub-poissonian twin beams via competing nonlinearities," *Phys. Rev. Lett.* **76**, 4815–4818 (1995).
14. M. A. M. Marte, "Nonlinear dynamics and quantum noise for competing $\chi^{(2)}$ nonlinearities," *J. Opt. Soc. Am. B* **12**, 2296–2303 (1995).
15. C. Cabrillo, J. L. Roldán, and P. García-Fernández, "Squeezing enhancement by competing nonlinearities: almost perfect squeezing without instabilities," *Phys. Rev. A* **56**, 5131–5134 (1997).
16. K. V. Kheruntsyan, G. Yu. Kryuchkyan, and K. G. Petrosyan, "Controlling instability and squeezing from a cascaded frequency doubler," *Phys. Rev. A* **57**, 535–547 (1998).
17. P. Tombesi and H. P. Yuen, "Enhanced squeezing in an optically bistable 2-photon medium," in *Coherence and Quantum Optics V*, L. Mandel and E. Wolf, eds. (Plenum, New York, 1984).
18. P. Tombesi, "Oversqueezing via 4-order interaction," in *Quantum Optics IV*, J. D. Harvey and D. F. Walls, eds. (Springer, New York, 1986).
19. P. Garcia-Fernández, P. Colet, R. Toral, M. San Miguel, and F. J. Bermejo, "Squeezing resulting from a fourth-order interaction in a degenerate parametric amplifier with absorption losses," *Phys. Rev. A* **43**, 4923–4929 (1991).
20. C. Cabrillo, F. J. Bermejo, P. García-Fernández, R. Toral, P. Colet, and M. San Miguel, "Transient behavior of a parametric amplifier with an added fourth-order interaction," *Phys. Rev. A* **45**, 3216–3223 (1992).
21. C. Cabrillo and F. J. Bermejo, "Control of the squeezing spectrum by means of a fourth-order interaction," *Phys. Lett. A* **170**, 300–304 (1992).
22. C. Cabrillo and F. J. Bermejo, "Large quadrature squeezing at high intensities," *Phys. Rev. A* **48**, 2433–2436 (1993).
23. G. Yu. Kryuchkyan and K. V. Kheruntsyan, "Exact quantum theory of a parametrically driven dissipative anharmonic oscillator," *Opt. Commun.* **127**, 230–236 (1996).
24. K. V. Kheruntsyan, D. S. Krahmer, and K. G. Petrossian, "Wigner function for a generalized model of parametric oscillator: phase-space tristability, competition and nonclassical effects," *Opt. Commun.* **139**, 157–164 (1997).
25. A. G. White, J. Mlynek, and S. Schiller, "Cascaded second-order nonlinearity in an optical cavity," *Europhys. Lett.* **35**, 425–430 (1996).
26. M. J. Collett and R. B. Levien, "Two-photon-loss model of intracavity second-harmonic generation," *Phys. Rev. A* **43**, 5068–5072 (1991).
27. S. Schiller, S. Kohler, R. Paschotta, and J. Mlynek, "Squeezing and quantum nondemolition measurements with an optical parametric amplifier," *Appl. Phys. B* **60**, S77–S88 (1995).
28. M. J. Collet and C. W. Gardiner, "Squeezing of intracavity and travelling-wave light fields produced in parametric amplification," *Phys. Rev. A* **30**, 1386–1391 (1984).
29. C. W. Gardiner, *Quantum Noise* (Springer-Verlag, Berlin, 1991), Chap. 5.3.
30. S. Reynaud, C. Fabre, and E. Giacobino, "Photon noise reduction by passive optical bistable systems," *Phys. Rev. A* **40**, 1440–1446 (1989).
31. C. Fabre, E. Giacobino, and A. Heidmann, "Squeezing in detuned degenerate optical parametric oscillators," *Quantum Opt.* **2**, 159–187 (1990).
32. K. Kasai, G. Jiangrui, and C. Fabre, "Observation of squeezing using cascaded nonlinearity," *Europhys. Lett.* **40**, 25–30 (1997).
33. A. G. White, M. S. Taubman, and H.-A. Bachor, "Experimental test of modular noise propagation theory for quantum optics," *Phys. Rev. A* **54**, 3400–3404 (1996).
34. C. Sirtori, F. Capasso, and D. L. Sivco, "Resonant Stark tuning of second-order susceptibility in coupled quantum wells," *Appl. Phys. Lett.* **60**, 151–153 (1992).
35. J. Faist, C. Sirtori, F. Capasso, S.-N. G. Chu, L. N. Pfeiffer, and K. W. West, "Tunable Fano interference in intersubband absorption," *Opt. Lett.* **21**, 985–987 (1996).
36. H. Schmidt, K. L. Campman, and A. Imamoglu, "Tunneling induced transparency: Fano interference in intersubband transitions," *Appl. Phys. Lett.* **70**, 3455–3457 (1997).
37. J. Faist, F. Capasso, and L. N. Pfeiffer, "Controlling the sign of quantum interference by tunnelling from quantum wells," *Nature* **390**, 589–591 (1997).
38. H. Schmidt and A. Imamoglu, "Nonlinear optical devices based on a transparency in semiconductors intersubband transitions," *Opt. Commun.* **131**, 333–338 (1996).
39. S. Schiller, G. Breitenbach, and J. Mlynek, "Subharmonic-pumped continuous-wave parametric oscillator," *Appl. Phys. Lett.* **68**, 3374–3376 (1996).
40. S. Schiller, R. Bruckmeier, and A. G. White, "Classical and quantum properties of the subharmonic pumped parametric oscillator," *Opt. Commun.* **138**, 158–171 (1997).
41. J. L. Sorensen and E. S. Polzik, "Internally pumped sub-threshold OPO," *Appl. Phys. B* **66**, 711–718 (1998).
42. A. G. White, P. K. Lam, and H.-A. Bachor, "Classical and quantum signatures of competing $\chi^{(2)}$ nonlinearities," *Phys. Rev. A* **55**, 4511–4515 (1997).